16th Australasian Fluid Mechanics Conference
Crown Plaza, Gold Coast, Australia
2-7 December 2007

# Simulations of Flow in a Solar Roof Collector Driven by Natural Convection.

**Tan Boon Thong, Lew Mai Quaan and Ong Kok Seng**

School of Engineering,
Monash University Sunway Campus, Malaysia.

**Abstract**

The solar roof collector is modelled as a two dimensional air gap with one heated wall. The Boussinesq approximation is used to model the density variation. Four different air gap heights were simulated, namely 0.07m, 0.014m, 0,21m and 0.28m for a 2m long solar roof collector. The tilt angle of the solar collector was also varied between 15° and 55° from horizontal. Predictions of velocities and mass flow rates in the air-gap are presented together with streamlines showing air flow patterns. The simulations show that a 0.14m air gap height at higher inclination angles is optimal for ventilation.

## Introduction

The hot and humid tropical weather in Malaysia coupled with the high population density in urban areas creates an unpleasant environment in houses. Mechanical ventilation and air conditioning have traditionally been used to improve the living environment. The rising cost of energy together with the environmental impact makes these options less attractive especially for lower income families. The solar roof collector studied in this paper is a cheap and simple way of providing natural ventilation for low cost homes. The design concept is presented in Figure 1. The top plate, which is usually made of steel sheets, is heated by solar radiation. Heat is transferred to the air in the gap via conduction and convection. The hot air in the air gap rises and this draws air from inside the house. Fresh air from outside the dwelling will then replace the air drawn out by the collector.

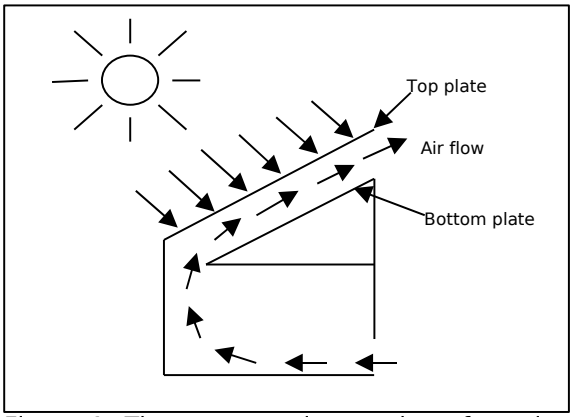


Figure 1: The conceptual operation of a solar roof collector.

The principal of operation of this device is similar to the Trombe wall. A Trombe wall usually uses a side wall of the structure. Glazing is sometimes used on the outer wall to allow solar radiation to directly heat the air in the cavity and the Trombe (inner) wall. Hocevar and Caperson [1] have measured the velocity profiles and mass flow rates in this configuration for various air gap sizes. Akbarzadeh et. al. [2] has done flow visualisation for various gap sizes. Hirunlabh et. al [3] studied the ventilation produced when a metallic surface for the exterior wall was used. Mathur et. al.[4] showed the importance of the chimney height in increasing ventilation rates. Simple theoretical models for Trombe walls are presented in Ong and Chow[5].

It is more practical to incorporate the solar roof collector into a low cost single story structure compared to a Trombe wall. This configuration is expected to collect more solar radiation in low structures without changing the overall architecture of the dwelling. The performance of a concrete tiled solar roof collector has been studied by Khedari et. al. [6]. Mathur et. al [7] studied the effect of inclination angle of solar roof collectors. The simulations presented here complement the experimental study presented in Ong et al. [8] and Ong et. al [9]. The parameters chosen for this study are shown in Figure 2 and are estimated based on their experimental setup.

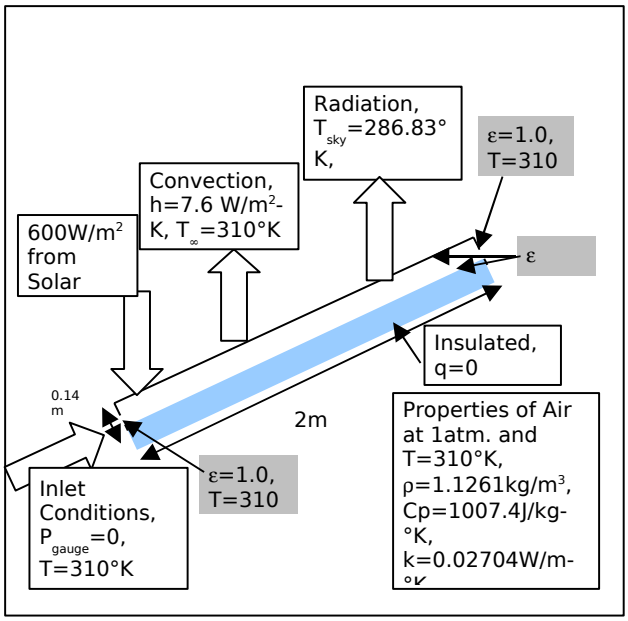

Figure 2: Parameters used in the numerical simulations.

The operating conditions show in Figure 2 are chosen to match experimental conditions in Malaysia at midday when solar radiation is at its highest. The properties of air are fixed at 1 atmosphere and 310°K (37°C). Ambient air temperatures usually reach this level during midday. The inlet conditions are therefore set to 1 atmosphere and 310°K. The pressure at the outlet is also set to 1 atmosphere and for cases where there is backflow at the outlet; the incoming air is also set to be at 310°K. Solar radiation on a horizontal surface reached 800W/m$^2$ during the experimental study [8.9]. The simulations used a reduced level of 600W/m$^2$ to roughly approximate the reduction in solar radiation due to the inclination of the exposed surface. The convection coefficient on the outside of the heated surface is calculated using the correlation for outdoor wind [10] which is, h(W/m$^{2\circ}$ K) =5.7+3.8U(m/s), and the wind velocity is estimated to be U=0.5m/s. The heated surface radiates heat back to the sky and the sky temperature is estimated using the correlation $T_{sky}$=0.0572 $T_{ambient}^{1.5}$ [11]. When the ambient temperature is $T_{ambient}$=310°K, the sky temperature is estimated to be $T_{sky}$=286.83°K. Both the top plate and the bottom plate are made of corrugated steel sheets. The emissivity on both sides of the top plate and the top side of the bottom plate is assumed to be ε=0.95. The bottom side of the bottom plate is assumed to be perfectly insulated. Radiation between the air gap and the outside environment can occur at the entrance and exit of the air gap. To account for this, the emmisivity and radiating temperature of the outside environment on both the inlet and outlet end of the air gap are set at 1.0 and 310°K respectively.

**Numerical Method.**

Simulations were performed using the commercial software Fluent. The flow is assumed to be two-dimensional, steady and laminar. These assumptions are based on the low air speeds in the air gap and the living space shields the inlet stream from atmospheric disturbances. The Boussinesq approximation is used to estimate the effect of density variation with temperature. This is valid for this study because the temperature variation is typically less than 20°K. The "surface to surface" radiation model is used to account for heat transfer between the top and bottom plate and between the plates and the inlet and outlet openings.

The momentum, continuity and energy equation are solved using the coupled solver. Initially the first order upwind scheme was used to get an approximate solution. This solution is then used as the initial conditions for the second order upwind solver. Several monitoring points near critical locations notably near the top plate and outlet area were used to check for the convergence of the solution. The courant number was lowered as the solution converged in order to avoid oscillatory solutions.

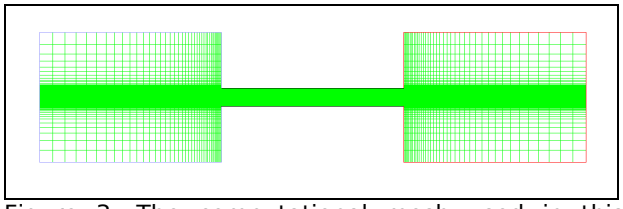

Figure 3: The computational mesh used in this simulation.

The computational mesh used in this study is shown in Figure 3. The computational domain is placed horizontally and various inclinations are modelled by varying the direction of gravity. The computational domain is expanded around the inlet and outlet area so as to minimize the effect of the computational boundaries on the solution. All boundaries around the expanded area on the inlet/outlet side are set to the inlet/outlet pressure boundary conditions. The value for pressure on the inlet/outlet boundary is set to atmospheric pressure. The normal velocity gradients are set to zero on all inlet/outlet boundaries.

Figure 4 shows a zoomed in view of the computational grid across the air gap. The mesh is compressed towards the solid boundaries in order to accurately capture the developing boundary layers. A total of 100 cells were placed across the air gap. A total of 200 cells were evenly placed along the 2m air gap.

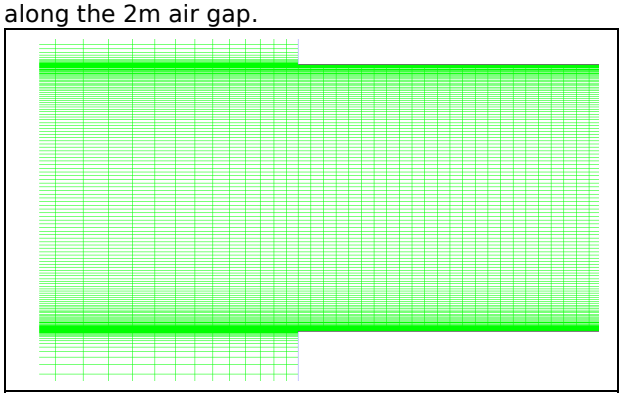

Figure 4: A close up view of computation map across the air gap.

**Results**

**Comparison with Experimental Findings**

Experiments were conducted using an air gap of 0.14m and with an inclination angle of 25° [8,9]. The temperature profile at 1.7m from the inlet was measured at 5 different stations across the air gap. A plot of the temperature profile measured during the middle of the day when solar radiation is at its peak is plotted in Figure 5. The corresponding simulated temperature profile is also plotted for comparison.

These results show that the thermal boundary layer is less than 0.4m from the top plate. Outside this region, the temperature is approximately constant

and equal to the ambient temperature. Although there is only a small difference between the experimental and simulated data, there is limited data near the top plate. Plans are currently underway to improve the experimental setup so that more data can be collected for comparisons.

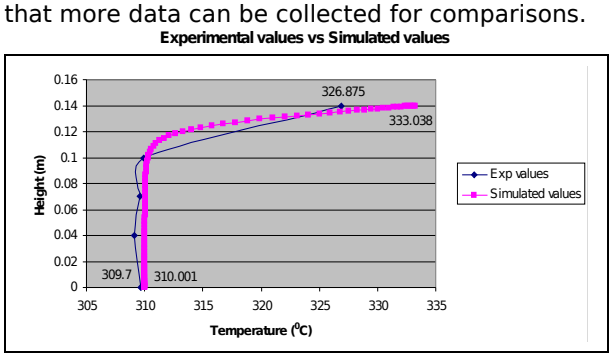


Figure 5: A comparison between the temperature profile across the air gap.

## Effects of Inclination Angle and Gap Width

Figure 6 shows the mass flow rate per unit width predicted for a range of gap heights between 0.07m to 0.28m at inclination angles of 15°, 25°, 35° and 55°. All cases show an increase in mass flow rate when the gap height is increased from 0.07m to 0.14m. Khedari et. al. [6] also showed experimentally that increasing the air gap from 0.08m to 0.14m resulted in an increase in ventilation. The mass flow rate decreases in all cases except for the case with a 55° inclination angle when the gat height is further increased. The next section will show that this is caused by the hot jet stream near the top plate drawing air in from the outlet. The backflow at the outlet of the air gap reduces the total mass transfer of air through the air gap.

These results show that a high inclination angle improves ventilation. This can be explained by buoyancy effects being stronger when the gap is closer to vertical. In these simulations, the amount of radiated heat to the top plate was fixed at 600W/m$^2$. In reality, higher inclination angles would result in less solar radiation on the top plate. It is therefore expected that the mass flow rate may be less than those predicted here at higher inclination angles. Mathur et. al [7] showed that high inclination angles between 40°-60° depending on latitude were optimal for ventilation purposes. These high inclination angles are not favourable for this particular application because of architectural and economic reasons.

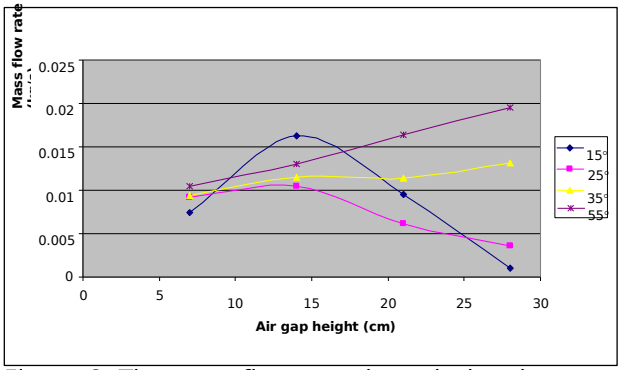


Figure 6: The mass flow rate through the air gap as a function of air gap height at various inclination angles.

## Flow Visualisation

The streamline plot for the case with a 0.14m air gap and a 25° inclination angle is shown in Figure 7. The plot shows that the flow from the inlet on the left converges towards the top wall. The top wall is heated by solar radiation. This heat is transmitted to the air close to the top wall. Buoyancy forces drive the heated air toward the outlet at the right side which is at a higher elevation. This volume is then filled by the incoming stream at the inlet. This process results in a jet of hot air close to the top wall leaving the air gap.

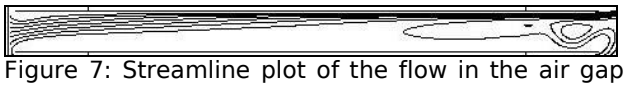

Figure 7: Streamline plot of the flow in the air gap with a height of 0.14m and an inclination angle of 25°.

The streamline plot shows that the hot jet occupies only a fraction of the air gap. This jet of air accelerates as it approaches the outlet and velocities within this jet can reach around 0.4m/s. When the jet is closer to the outlet, the preference switches from drawing inlet air to drawing air from the outlet opening of the air gap. This process hinders the ventilation capability of this device. Results from the earlier subsection has shown that mass flow rates actually drops when air gap height in increased. The decrease in mass flow rate is a result of increasing backflow at the outlet opening of the air gap.

The computational domain extends some distance away from the exit of air gap as seen in Figure 2. This precaution was taken to reduce the artificial effects of the outflow boundary on the flow pattern in the air gap. This backflow in the air gap will have to be further investigated before ruling out the possibility that it is a manifestation of the boundary condition. Experimental results have consistently showed that the temperature of the top plate along the length of the air gap actually decreases closer to the exit of the air gap [9]. Although the simulations have not reproduces this phenomenon, backflow from the outlet may contribute to this cooling effect. Research is currently ongoing with

the aim of collecting more details on the flow within the air gap.

**Conclusion**

The natural convection driven flow is simulated for a typical solar roof collector operating at peak mid-day conditions in Malaysia. Results show that the amount of ventilation can be increased with increasing inclination angles. Except for the highest inclination angle, the simulations have shown that air gap heights past 0.14m actually reduce the mass flow rate. This is caused by the hot jet close to the top wall in the air gap drawing air from the outlet. The reverse flow near the outlet reduces the mass flow rate through the air gap.

**References**


[1] Hocevar, C. J. & Casperson, R. L., Thermocirculation data and instantaneous efficiencies for Trombe walls. Proc. 4th National Passive Solar Conference, Kansas City, Missouri, USA, 163-167, 1979.

[2] Akbarzadeh, A., Charters, W. W. S. & Lesslie, D. A., Thermocirculation characteristics of a Trombe wall passive test cell. Solar Energy, **28**, 461-468, 1982.

[3] Hirunlabh, J., Kongduang, W., Namprakai, P., & Khedari, J., Study of natural ventilation of houses by a metallic solar wall under tropical climate, Renewable Energy, **18**, 109-119, 1999.

[4] Mathur, J., Bansal, N. K., Mathur, S., Jain, M. & Anupma, Experimental investigations on solar chimney for room ventilation. Solar Energy, **80**, 927-935, 2006.

[5] Ong, K. S. & Chow, C. C., Performance of a solar chimney. Solar Energy, **74**, 1-17, 2003.

[6] Khedari J., Mansirisub, W., Chaima, S., Pratinthong, N. & Hirunlabh, J., Field measurements of performance of roof solar collector. Energy and Buildings, **31**, 171-178, 2000.

[7] Mathur, J., Mathur, S & Anupma., Summer performance of inclined roof solar chimney for natural ventilation, Energy and Buildings, **38**, 1156-1163, 2006.

[8] Ong, K. S., Performance of a natural convection solar air heater. J. Energy, Heat and Mass Transfer, **27**, 229-246, 2005.

[9] Ong, K. S., Tan, B. T., Joe, R. and Tan, K. S., Feasibility of solar passive cooling. Int. Symposium & Exhibition on Sustainable Energy & Environment, Malaysia, 2006.

[10] McAdams W.H., Heat Transmission, New York: McGraw-Hill, 1954.

[11] Swinbank, W.C., Long-wave radiation from clear skies, Q.J.R. Meteorological Society, 1963, **89**, 339.